J Mater Sci (2010) 45:3289–3299
DOI 10.1007/s10853-010-4342-6

Synthesis and characterizations of Cd^{2+}, Pb^{2+} and Sr^{2+} containing divinyl monomers and their melt grafting reaction with LLDPE: an FTIR approach

R. Anbarasan · V. Dhanalakshmi · M. Sudha

Received: 11 January 2010 / Accepted: 22 February 2010 / Published online: 9 March 2010

Abstract The divinyl esters containing divalent metal ions like Cd, Pb and Sr are synthesized and characterized by various analytical tools such as Fourier transform infrared spectroscopy (FTIR), differential scanning calorimetry, thermogravimetric analysis and X-ray diffractogram. Further, it is subjected to melt graft functionalization reaction with linear low-density poly(ethylene) (LLDPE) at 160 °C under inert atmosphere. The FTIR–relative intensity method is used to calculate the % grafting of metal esters onto LLDPE backbone. The results are critically compared and discussed. Suitable reaction mechanism is proposed.

Introduction

Poly(ethylene)s (PEs) are valuable materials for commercial applications because of their low price and wide requirements for different application purposes. Despite their good processing properties, the non-biodegradable character of PEs prevents their usage in a wide range. This non-biodegradability of PE is due to the absence of polar or hydrolysable groups in its backbone. This problem can be outwitted by the graft functionalization of metal containing acrylate monomers onto PE backbone in their molten state. The advantages of this method are (1) eco-friendly, (2) susceptible to easy attack by various soil living microorganisms, (3) increase in mechanical and thermal properties. Metal salts are synthesized and characterized by different authors. In 1989, Savostyanov et al. [1] studied the kinetics of radiation-induced graft polymerization of Mn, Cr, Fe, Co, Ni and Cu acrylates onto PE surface. Solid-state polymerization of γ-ray-irradiated calcium acrylate was reported by Costaschuk et al. [2]. Further the polymer was characterized by ESR spectra. Solid-state polymerization of ferrocenyl ethylacrylate and ethylmethacrylate report is available in the literature [3, 4]. Solution copolymerization of styrene with acrylates of Mg, Ca, Sr and Ba was reported in 1989 by Cronosvski and Wojtczak [5]. Zinc dimethacrylate-reinforced EPDM rubber was reported with improved mechanical properties [6]. Peroxide-mediated copolymerization of zinc dimethacrylate and 2-(*N*-ethyl perfluoro octanesulphonamido) ethyl acrylate was synthesized and characterized by transmission electron microscopy, dynamical mechanical analysis and surface tension methods [7]. Other authors also synthesized and characterized the metal acrylate esters [8–15]. Low-temperature synthesis of La, Mn and Sr acrylates was synthesized and characterized [16]. Cd acrylate surface-coated CdS [17] and CdSe [18] quantum dot report is available in the literature. In 2008, Huang et al. [19] studied the toughening effect of maleic anhydride grafted linear low-density poly(ethylene) (LLDPE). By thorough literature survey, we found that few reports are available based on the synthesis and characterizations of Cd, Pb and Sr acrylates and methacrylates. In this investigation we successfully synthesized and melt grafted the same metal salts onto LLDPE backbone by thermolysis method in the presence

R. Anbarasan (✉)
Department of Mechanical Engineering, MEMS Thermal Control Lab, National Taiwan University, Taipei 10617, Taiwan, ROC
e-mail: anbu_may3@yahoo.co.in

V. Dhanalakshmi
Department of Polymer Technology, KCET, Virudhunagar 626 001, Tamil Nadu, India

M. Sudha
Department of Chemistry, N.S. College of Arts and Science, Theni 625 531, Tamil Nadu, India

of a free radical initiator under inert atmosphere at 160 °C for the first time.

After the melt functionalization process, the amount of ester grafted onto LLDPE backbone can be determined by chemical as well as analytical methods. In general, the chemical method produced the environmental pollution because of utilization of expensive, toxic and hazardous solvents. The analytical methods are eco-friendly and inexpensive with more accuracy. For these reasons, we preferred the analytical method to find out the amount of ester grafted onto LLDPE backbone, particularly, Fourier transform infrared spectroscopy (FTIR) method. FTIR spectrometer is a useful tool in various science and engineering fields, because of its high sensitivity or detectivity towards traces amount of sample, low noise-to-signal ratio and this method is an easy and inexpensive one. FTIR spectroscopy is used for both qualitative [20–23] and quantitative [24–36] analysis. By thorough literature survey, we could not find any report based on the FTIR kinetics of melt functionalization of the above-mentioned esters onto LLDPE backbone. In this investigation, for the first time, we are reporting about the melt functionalization of the above-mentioned metal salts with LLDPE and further characterized by FTIR–relative intensity (RI) method-based kinetics.

Experimental

Materials

Carbonates of Cd, Pb and Sr were purchased from SD Fine Chemicals, AR grade, India. Acrylic acid and methacrylic acid (CDH Chemicals, India) were purchased and used after distillation under vacuum. Linear LLDPE (Rayson, India, $M_w = 100000$ Da) was purchased and purified by the procedure followed in our earlier publication [33]. Toluene (Chemspure, AR, India) and acetone (Merck, India) were used as-received. Dicumyl peroxide initiator (DCP, Across Chemicals, UK) and cyclohexane (Paxy chemicals, AR, India) were used as-received.

Synthesis of cadmium diacrylate (Cd DA)

10 g of $CdCO_3$ was dissolved in 200 mL of slightly acidic double distilled water in a three-necked round bottom (RB) flask. 20 mL of acrylic acid was added drop-by-drop to the $CdCO_3$ solution followed by 0.03 g of antimony trioxide, the esterification catalyst, to catalyze the metal salt formation process. The contents were sparged with nitrogen gas to create an inert atmosphere inside the flask. The RB flask was connected to a water condenser and the solution was boiled for 3 h continuously, with vigorous stirring at 90 °C. Finally, the precipitate {Cd DA} was washed with acetone and the sample was dried, weighed and stored in a zipper bag. The same procedure was adopted for the synthesis of other metal salts too.

Purification of LLDPE

5 g of LLDPE pellet sample was dissolved in 100 mL of toluene solvent at 140 °C for 3 h in order to remove the antioxidants, added during its long storage process. Once all the LLDPE powder samples were dissolved in toluene, then cool it and 800 mL of acetone was added to precipitate the LLDPE [33]. Filtered the contents and dried at 60 °C for 24 h under vacuum. The dissolution and precipitation process were repeated three times to further purify the LLDPE. Finally, the dried samples were weighed and stored in a zipper bag.

Synthesis of LLDPE-*g*-Cd DA

1 g of pure LLDPE powder sample was added with 1 wt% of Cd DA in 25 mL of cyclohexane–dichloromethane (1:9 v/v) solvent mixture in a 100-mL beaker with mild stirring. The solvent mixtures were used to distribute the DCP and Cd DA onto LLDPE backbone uniformly, otherwise agglomeration occurred. Then 1 wt% of DCP was mixed with the content of the beaker and the stirring was continued for 1 h. In this investigation, both DCP and esters or Cd DA were used in equal concentrations, particularly with 1:1 ratio, after many trial experiments. After 1 h of mixing, the solvent was removed by rotary evaporation. The reaction mixture was transferred into a test tube reactor and de-aerate for 30 min with sulphur-free nitrogen gas. After degassing, the temperature of the reactor was kept at 160 °C for 2.5 h without stirring. After functionalization reaction was completed, the reactor was removed from the oil bath, cooled to room temperature and the functionalized LLDPE samples were collected and cut into small pieces. These were put in toluene at 140 °C for 30 min for the isolation purpose. The functionalized, non-cross-linked samples dissolved in toluene, whereas the functionalized cross-linked samples did not. The dissolved samples were re-precipitated by adding 600 mL of acetone and the cross-linked samples were isolated. The non-cross-linked sample was collected and dried under vacuum at 60 °C. After drying, the sample was weighed and stored in a zipper bag. FTIR spectrum was obtained and quantitative calculations have done with the non-cross-linked, functionalized polymers. The same grafting procedure was followed for other metal esters too.

Characterizations

FTIR spectra were recorded using 8400 S Shimadzu FTIR spectrometer, Japan, by KBr pelletization method for 7 mg

of samples in the form of pellet from 400 to 4000 cm^{-1}. In order to avoid error while recording FTIR spectrum, the corrected peak area was considered. To cross-check the corrected peak area values, the FTIR spectra were recorded for the same sample disc in different parts. After proper baseline correction with the aid of FTIR software, again one can get the same corrected peak area values. FTIR spectrum was recorded for three times for the same sample disc, one can get the same and repeated corrected peak area values. The FTIR spectrum was recorded without predicting the lower and upper limits of peaks, because the software itself predicted exactly the lower and upper limits to nullify the errors. In such a way the errors were nullified. Further one can cross-check the efficiency of FTIR software by manually predicting the lower and upper limits and the corrected peak area was determined. In this case one can get the same corrected peak area value as reported previously (without predicting the lower and upper peak limits). For the quantitative determination of % ester grafting, the following corrected areas of the peaks, which were assigned at 1730 (C=O form) and 721 (C–H out of plane bending vibration) cm^{-1} were determined and the RI was calculated as follows

$$\text{Relative intensity of ester carbonyl } \left(\text{RI}_{[\text{C=O/C–H}]}\right) = A_{1730}/A_{721} \quad (1)$$

$$\%\ \text{Ester grafting} = \frac{\text{RI}_{[\text{C=O/C–H}]} \times W}{C \times 1.5} \times 100 \quad (2)$$

where W is the weight of non-cross-linked ester grafted polymer taken for FTIR study, C is the wt% of peroxide used and 1.5 is the proportionality constant as mentioned in our earlier publication [33]. The % cross-linking was determined by using the following formula:

$$\%\ \text{Cross-linking} = \frac{[\text{Weight of polymer taken for functionalization}] - [\text{Weight of non-cross-linked polymer obtained after functionalization}]}{\text{Weight of polymer taken for functionalization}} \times 100 \quad (3)$$

Thermogravimetric analysis (TGA) was recorded using Universal V4.3A TA instrument, Japan, under air atmosphere from room temperature to 800 °C at the heating rate of 10 °C/min. Differential scanning calorimetry (DSC) of the sample was recorded using Universal V4.3A TA instrument under nitrogen atmosphere at the heating rate of 10 °C/min from room temperature to 300 °C. X-ray diffractogram (XRD) was recorded using Rigaku Rint 2000 (Japan) diffractometer at room temperature with Cu Kα1 radiation from the 2θ value of 2° to 60°. The voltage and current of X-ray tubes were 40 kV and 100 mA, respectively.

Results and discussion

This section is divided into two parts namely (1) synthesis and characterizations of metal containing monomers and (2) melt grafting of metal containing monomers onto LLDPE backbone.

Synthesis and characterizations of metal salt containing monomers

FTIR study

The FTIR spectra of metal esters are shown in Fig. 1. Figure 1a indicated the FTIR spectrum of Cd DA. The important peaks are characterized below. A broad peak around 3430 cm^{-1} is due to the OH stretching of water molecules attached with the central metal ion. Presence of water molecules in the metal esters will be further confirmed in the DSC and TGA analysis. The C–H symmetric and anti-symmetric stretching are observed at 2835 and 2992 cm^{-1}, respectively. A small peak at 1729 cm^{-1} is depicted the carbonyl stretching vibration of Cd DA. A small hump at 1665 cm^{-1} is corresponding to the C=C stretching. A sharp peak at 1636 cm^{-1} is responsible for the bending vibration of water molecules or $CO_2{}^{-}M^{+}$ linkage. The C–H bending vibration is seen at 1526 cm^{-1}. The metal ester linkage can be observed at 1048 cm^{-1}. The C–H out of plane bending vibration and metal–oxide stretching are appeared at 833 and 674 cm^{-1}, respectively. The same peaks are also seen for other metal esters (Fig. 1b–f) corresponding to cadmium dimethacrylate (Cd DMA), lead diacrylate (Pb DA), lead dimethacrylate (PB DMA), strontium diacrylate (Sr DA) and strontium dimethacrylate (Sr DMA), respectively.

DSC analysis

Figure 2 represented the DSC heating scan of acrylates and methacrylates of metal salts. Figure 2a exhibited the DSC

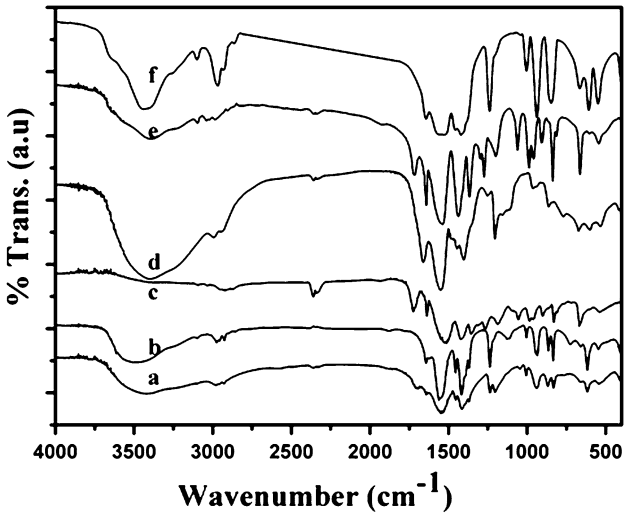

Fig. 1 FTIR spectra of *a* Cd DA, *b* Cd DMA, *c* Pb DA, *d* Pb DMA, *e* Sr DA, *f* Sr DMA

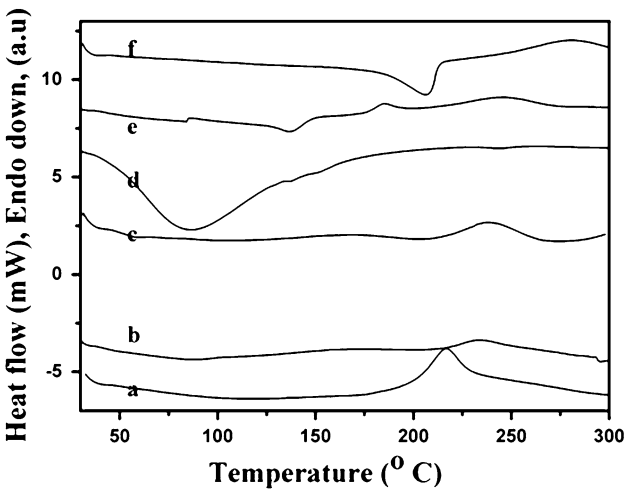

Fig. 2 DSC of *a* Cd DA, *b* Cd DMA, *c* Pb DA, *d* Pb DMA, *e* Sr DA, *f* Sr DMA

heating scan of Cd DA. It showed one broad endothermic peak and one sharp exothermic peak at 117 and 216.6 °C, respectively. The endothermic peak is due to the removal of chemisorbed [33] water molecules ($T_{d.w}$) and the exothermic peak is due to the cold crystallization temperature ($T_{c.c}$) of Cd DA. The presence of water molecules in the metal ester was already confirmed by the FTIR spectrum. Appearance of $T_{c.c}$ confirmed the semi-crystalline nature of Cd DA. Up to 300 °C the system did not show the melting (T_m) endothermic peak. This suggested that the T_m may appear at the still higher temperature. Table 1 listed the DSC data of this system.

The Cd DMA also showed the same type of thermogram (Fig. 2b). The $T_{d.w}$ is appeared at 87.9 °C and the $T_{c.c}$ is appeared at 233.5 °C. The reduction in $T_{d.w}$ and increase in

Table 1 DSC and TGA data of metal salts

System	$T_{d.w}$ (°C)	$T_{c.c}$ (°C)	Wt% above 750 °C
Cd DA	117.2	216.1	33.5
Cd DMA	87.9	233.5	46.9
Pb DA	103.6	237.7	54.5
Pb DMA	84.8	–	15.6
Sr DA	136.6	246.2	42.9
Sr DMA	205.7	280.7	50.4

$T_{c.c}$ are due to the increase in hydrophobic nature of Cd DMA. The methyl group in the Cd DMA increased the hydrophobic character and hence removal of chemisorbed water molecules at the earliest temperature. The same methyl group also influenced the $T_{c.c}$ by the way of slight increase in molecular weight and increase in conformational energy due to the bulky methyl substituent. This system also failed to exhibit T_m in the given temperature range. The increase in $T_{c.c}$ might be resulted with increase in T_m of Cd DMA. In comparison, the Cd DMA showed higher $T_{c.c}$ value due to the presence of methyl substituent in the Cd DMA.

Figure 2c represented the DSC heating scan of Pb DA. The present system exhibited one endothermic peak at 103.6 °C and one exothermic peak at 237.7 °C due to $T_{d.w}$ and $T_{c.c}$, respectively. Here also the T_m was not appeared in the given temperature range. This inferred that Pb DA came under semi-crystalline system with higher $T_{c.c}$ value. Figure 2d indicated the DSC heating thermogram of Pb DMA. It showed only one broad endothermic peak at 84.8 °C due to $T_{d.w}$. This system did not show the $T_{c.c}$ or T_m in the given temperature range. Reduction in $T_{d.w}$ suggested that the Pb DMA was more hydrophobic than Pb DA. In comparison, the $T_{d.w}$ of Pb DMA is lower than that of Pb DA due to the increase in hydrophobic character of Pb DMA. Figure 2e showed the heating scan of Sr DA. As usual, it explored one endothermic peak (at 136.6 °C) due to $T_{d.w}$ and one exothermic peak at 246.2 °C due to $T_{c.c}$. Here both $T_{d.w}$ and $T_{c.c}$ values are higher than that of the previous Cd and Pb salts. This inferred that Sr DA is thermally stable than Cd and Pb DAs. Figure 2f exhibited the DSC heating scan of Sr DMA. It showed one endothermic peak at 205.7 °C due to the $T_{d.w}$ and an exothermic peak at 280.7 °C due to $T_{c.c}$. The size and shape confirmed that this peak was corresponding to a $T_{d.w}$. In comparison, the Sr DMA yielded higher $T_{d.w}$ and $T_{c.c}$ values when compared with previous systems. In overall comparison, the Sr salts revealed the higher $T_{d.w}$ and $T_{c.c}$ due to the smaller in size of Sr atom with the outer most configuration of $5s^2$ with higher oxidation potential. Table 1 summarized the DSC data of all the systems.

TGA history

The thermal stability of Cd DA is shown in Fig. 3a. The thermogram showed a four-step degradation process. The first minor weight loss step up to 375 °C is due to the removal of moisture, physisorbed and chemisorbed water molecules. The second major weight loss step around 420 °C is associated with the dissociation of metal ester linkage. The third and fourth minor weight loss steps are corresponding to the degradation of acrylate ester linkage with the liberation of CO_2. Above 750 °C the system showed 33.5 wt% residue remained (Table 1). The thermograms are similar to that of the TGA of Ca DA and Ca DMA [33].

The TGA of Cd DMA is represented in Fig. 3b. The thermogram exhibited a 5-step degradation process. The first minor weight loss step below 100 °C is associated with the removal of moisture and physisorbed water molecules. The second minor weight loss step around 350 °C is accounted by the removal of chemisorbed water molecules. The third major weight loss step is appeared around 413 °C. This major weight loss step is depicted the dissociation of metal ester bond. The last two minor weight loss steps are corresponding to the dissociation and degradation of acrylate ester with the removal of CO_2 and CH_4 gas. The GPC analysis is under investigation in our lab. The first minor weight loss step in the TGA and the $T_{d.w}$ of DSC are co-inside with FTIR results. Moreover, above 750 °C it exhibited 46.9 wt% residue remained (Table 1). This explained that Cd DMA is more stable than Cd DA.

Figure 3c committed the TGA of Pb DA. The present system revealed the four-step degradation process. The first and second minor weight loss steps before 350 °C are associated with the removal of moisture, physisorbed and chemisorbed water molecules. The third major weight loss step around 400 °C is explained by the dissociation of metal ester bond. The fourth minor weight loss step is due to the degradation of acrylate ester linkage with the evolution of CO_2. After complete burning, it showed 54.5 wt% residue remained due to the formed metal oxide (Table 1). Figure 3d explained the TGA of Pb DMA. It showed a three-step degradation process. The first minor and the second major weight loss steps are associated with the removal of water molecules and dissociation of metal ester linkage, respectively. The third minor weight loss step is responsible for the degradation of acrylate ester group with simultaneous liberation of CO_2. Above 750 °C it gave 15.6 wt% residue. Due to the improper removal of water molecules from the sample, it showed lower % weight residue above 750 °C (Table 1). The TGA of Sr DA is mentioned in Fig. 3e. Again it showed a three-step degradation process. The important point noted here is the metal ester bond dissociation occurred around 500 °C. This is definitely greater than that of the TGA of previous systems. Above 750 °C it yielded 42.9 wt% residue remained (Table 1). Figure 3f revealed the TGA of Sr DMA. A three-step degradation process is observed here. Above 750 °C, 50.5 wt% residue remained (Table 1). In comparison, the Pb DA showed higher % weight residue remained above 750 °C among the metal diacrylates. Among the metal dimethacrylates, the Sr DMA exhibited higher % weight residue remained above 750 °C.

XRD profile

XRD of metal esters are represented in Fig. 4. Figure 4a, b shows the XRD of Cd DA and Cd DMA, respectively. Different crystal planes are observed in the diffractogram. The important ones are characterized below.

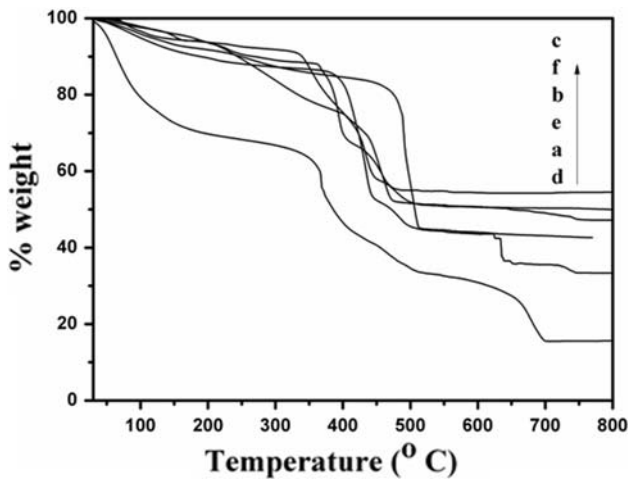

Fig. 3 TGA of *a* Cd DA, *b* Cd DMA, *c* Pb DA, *d* Pb DMA, *e* Sr DA, *f* Sr DMA

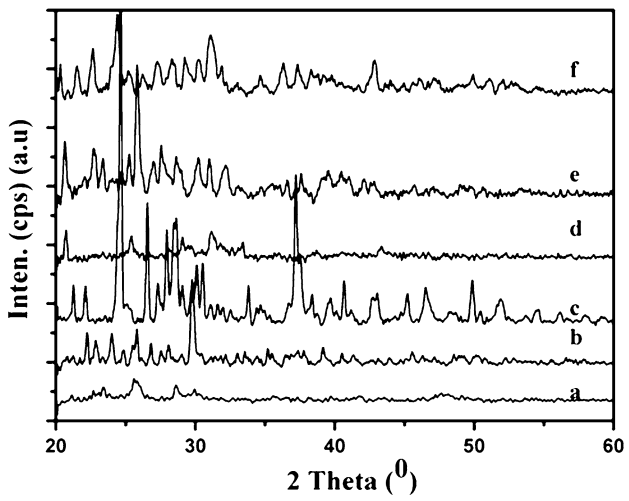

Fig. 4 XRD of *a* Cd DA, *b* Cd DMA, *c* Pb DA, *d* Pb DMA, *e* Sr DA, *f* Sr DMA

The $d_{111,\ 200,\ 220,\ 311,\ 222}$ are observed at 22.24, 28.69, 39.14, 45.32, and 47.69° respectively. This is in accordance with the literature report [18]. In comparison, the Cd DMA showed higher crystallinity than the Cd DA. Figure 4c, d shows the XRD of Pb DA and Pb DMA, respectively. Pb DA exhibited one sharp peak at the 2θ value of 24.6°. This confirmed the highly crystalline nature of Pb DA. Other crystal planes are also observed. In comparison, the Pb DA exhibited higher crystallinity than the Pb DMA. Figure 4e, f reveals the XRD of Sr DA and Sr DMA, respectively. Sr DA showed one sharp peak at 25.8°. In comparison, the Sr DA is having more crystal peaks than Sr DMA. In over all comparisons, the Pb DA showed the highest crystallinity among the metal ion containing divinyl monomers.

HRTEM report

Figure 5 shows the HRTEM images of Sr DMA. Figure 5a shows the broken layered structural arrangement of different crystal planes of Sr ions. The length of Sr stack in Sr DMA was found to be 15–20 nm. Figure 5b represents the agglomerated sphere-like structure of Sr DMA with the diameter of <5 nm. Sr DMA synthesized in this study is in nm size.

Melt grafting of metal containing divinyl monomers onto LLDPE backbone

FTIR study

Figure 6 enumerated the FTIR spectra of 1–5 wt% Cd DA loaded LLDPE system. Figure 6a reveals the FTIR spectrum of pristine LLDPE. The important peaks are characterized below. A broad peak around 2896 cm^{-1} is due to the anti-symmetric stretching. The C–H symmetric stretching vibration is observed at 2655 cm^{-1}. The C–H bending and out of plane bending vibration are seen at 1460 and 721 cm^{-1}, respectively. Figure 6b–f indicates the

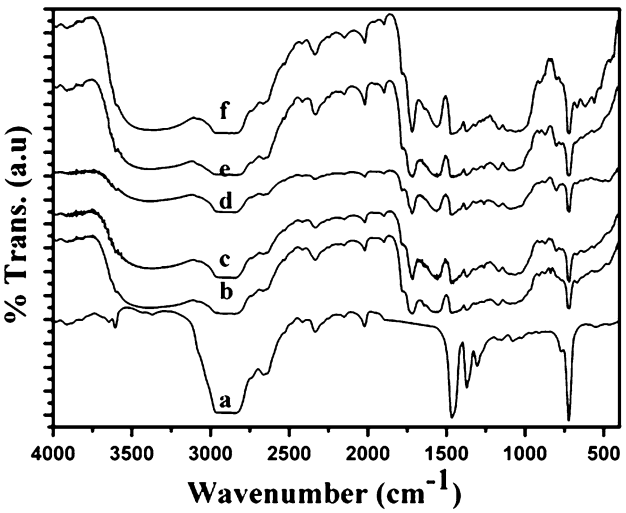

Fig. 6 FTIR spectra of LLDPE loaded with Cd DA at *a* 0 wt%, *b* 1 wt%, *c* 2 wt% , *d* 3 wt%, *e* 4 wt%, *f* 5 wt%

FTIR spectra of 1–5 wt% Cd DA-loaded LLDPE. The spectra showed some new peaks apart from the peaks of pristine LLDPE. They are characterized below. A broad peak around 3500 cm^{-1} is ascribed to the OH stretching of Cd DA. During the melt graft functionalization reaction, hydrogen transfer reaction occurred and resulted with acidification of part of Cd DA. Moreover, 2 mol of water is attached with central Cd ion. This is in accordance with our earlier publication [32]. The ester grafting can be confirmed by representing a peak at 1721 cm^{-1} due to the ester carbonyl group. The bending vibration of water and $CO_2^-M^+$ stretching is merged and observed as a broad peak at 1571 cm^{-1}. A broad peak around 1058 cm^{-1} is responsible for the ester C–O–C linkage. The Cd–O stretching is seen at 562 cm^{-1}. Appearance of these new peaks confirmed the chemical grafting of Cd DA onto LLDPE backbone.

The interesting point observed here is while increasing the % weight loading of Cd DA, the RI of [C=O/C–H] is

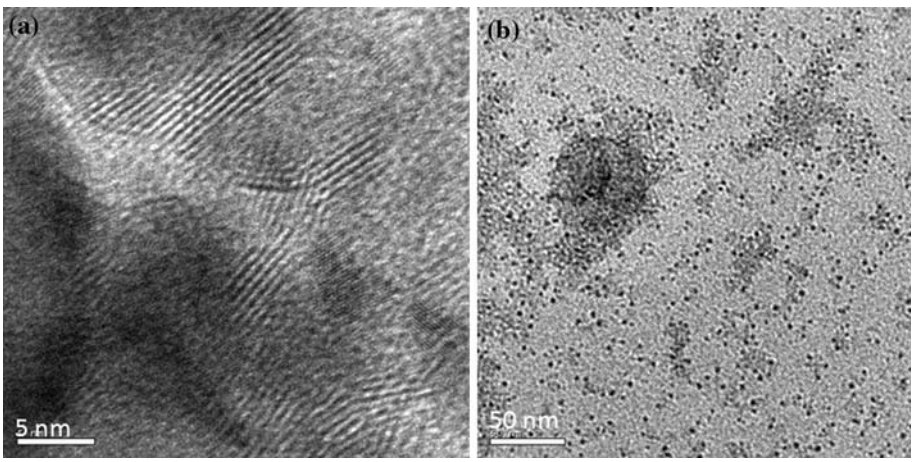

Fig. 5 HRTEM images of Sr DMA

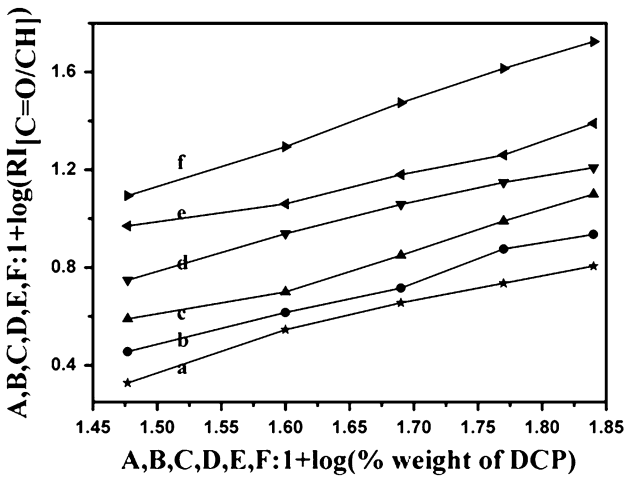

Fig. 7 Effect of (% weight of DCP) on $RI_{[C=O/C–H]}$ of *a* Cd DA, *b* Cd DMA, *c* Pb DA, *d* Pb DMA, *e* Sr DA, *f* Sr DMA systems

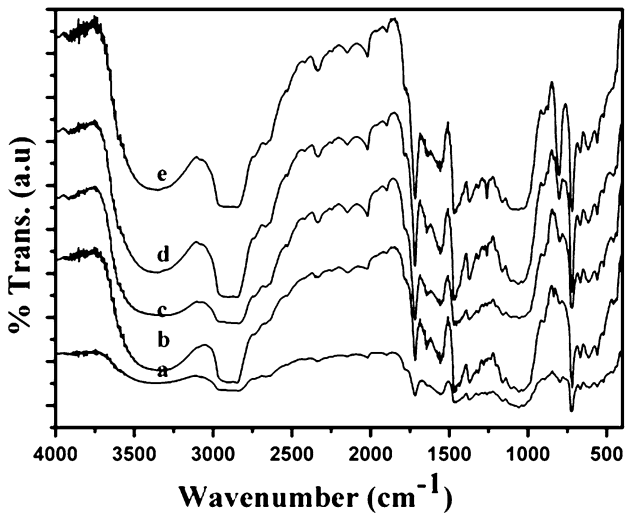

Fig. 8 FTIR spectra of LLDPE loaded with Cd DMA at *a* 1 wt%, *b* 2 wt%, *c* 3 wt%, *d* 4 wt%, *e* 5 wt%

also increased. This argued that the chemical grafting is increased with the increase in % weight loading of Cd DA. In this investigation the DCP and Cd DA were used in equal concentration. Figure 7a shows the plot of log(% weight of DCP) versus $\log(RI_{[C=O/C–H]})$. The plot showed a straight line with the slope value of 1.29, which declared the 1.25 order dependence of grafting reaction with respect to % weight of DCP. It means that 1.24 mol of DCP is required to functionalize 1 mol of LLDPE. The rate of functionalization reaction (R_f) can be written as follows: $R_f \propto (\%\text{ weight of DCP})^{1.29}$. The % grafting values are mentioned in Table 2. Recently, Anbarasan and co-authors [36] found similar type of results during the melt graft functionalization of mercapto esters with HDPE. The Cd DA contains two C=C double bonds. According to the order of functionalization reaction, one double bond of Cd DA was involved in functionalization reaction; the remaining one was as such. The presence of double bond even after melt functionalization could be confirmed by observing a peak at 1571 cm^{-1}. Hence a broad peak at 1571 cm^{-1} is due to the combination of C=C stretching, OH bending vibration, $CO_2^-M^+$ stretching vibrations. Hence, the grafting of Cd DA onto LLDPE backbone occurred through the cleavage of one C=C double bond. The competitive reaction during the melt graft functionalization reaction is the cross-linking reaction. Cross-linking is due to the coupling of LLDPE macroradicals. Table 2 indicated the % C.L values. The % C.L values increased with the increase in % weight loading of Cd DA.

Table 2 Effect of % weight of Cd salts on % grafting and % C.L

%Wt loading	Cd DA		Cd DMA	
	% Grafting	% C.L	% Grafting	% C.L
1	48.7	4.5	39.4	9.5
2	51.0	8.9	44.5	17.4
3	56.8	13.2	47.8	26.8
4	61.9	19.8	50.2	32.7
5	68.4	24.7	56.6	38.1

Figure 8 provides the FTIR spectra of Cd DMA-grafted LLDPE system. The DCP and metal ester concentrations were varied from 1 to 5 wt%. Here also one can observe the above-mentioned peaks. While increasing the % weight loading of Cd DMA, the RI of [C=O/C–H] is also increased. This is due to the more and more chemical grafting of Cd DMA onto LLDPE backbone. In order to find out the order of functionalization reaction, the following universal log–log plot was made. Figure 7b showed the plot of log(% weight of DCP) versus $\log(RI_{[C=O/C–H]})$ and the plot showed a straight line with the slope value of 1.35; $R_f \propto (\%\text{ weight of DCP})^{1.35}$. This claimed 1.50 order of melt functionalization reaction. This is in accordance with our earlier publication [33]. In the case of Cd DMA, 1.50 mol of Cd DMA is required to functionalize 1 mol of LLDPE. The % grafting values and % C.L values are listed in Table 2. In critical comparison, Cd DA system exhibited higher % grafting values due to the absence of steric effect. The Cd DMA system revealed the higher % C.L values due to slow rate of formation of Cd DMA radicals.

The FTIR spectra of 1–5 wt% Pb DA-loaded LLDPE is shown in Fig. 9. While increasing the % weight of Pb DA, the RI of [C=O/C–H] is also increased. At higher % weight of loading of Pb DA, the carbonyl stretching and the bending vibration of water molecules were merged and the carbonyl peak was observed like a hump. The remaining peaks are similar to that of Cd DA–LLDPE system. The order of functionalization reaction can be determined by plotting log(% weight of DCP) versus $\log(RI_{[C=O/C–H]})$

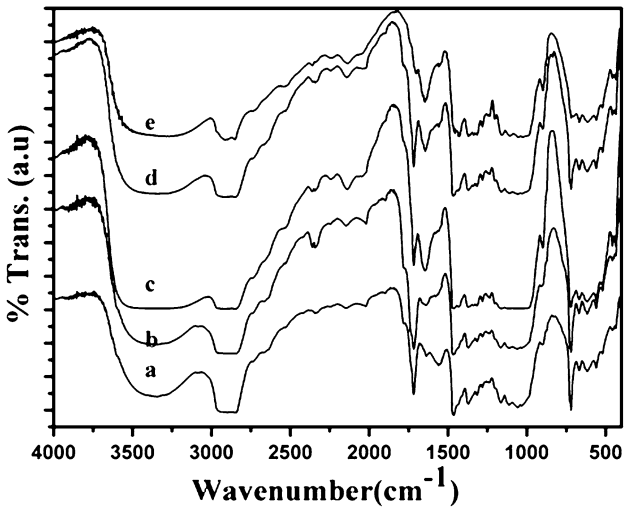

Fig. 9 FTIR spectra of LLDPE loaded with Pb DA at *a* 1 wt%, *b* 2 wt%, *c* 3 wt%, *d* 4 wt%, *e* 5 wt%

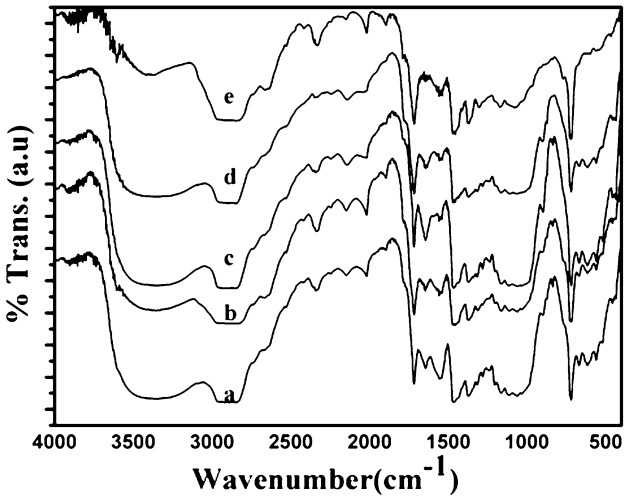

Fig. 10 FTIR spectra of LLDPE loaded with Pb DMA at *a* 1 wt%, *b* 2 wt%, *c* 3 wt%, *d* 4 wt%, *e* 5 wt%

(Fig. 7c). The plot exhibited a straight line with a slope value of 1.44, which concluded the 1.50 order of functionalization reaction, i.e. $R_f \propto (\%\ \text{weight of DCP})^{1.44}$. 1.50 mol of Pb DA is required to functionalize 1 mol of LLDPE. This is in accordance with literature report [33]. The % grafting and % C.L values are mentioned in Table 3. Figure 10 exhibited the FTIR spectra of 1–5 wt% Pb DMA-loaded LLDPE system. The RI of [C=O/C–H] is increased with simultaneous increase in % weight loading of Pb DMA. Figure 7d indicated the plot of log(% weight of DCP) versus log($RI_{[C=O/C-H]}$). The plot showed a straight line with the slope value of 1.27, i.e. $R_f \propto (\%\ \text{weight of DCP})^{1.27}$. 1.25 mol of Pb DMA is required to functionalize 1 mol of LLPDE. The % functionalization and % C.L values are represented in Table 3. In comparison, the % grafting values are greater than that of % C.L. Pb DA system exhibited higher % functionalization values due to the absence of steric effect and the Pb DMA system revealed higher % C.L values due to the presence of steric effect and slow production of Pb DMA radicals. By comparing Cd and Pb systems, the Cd system yielded higher % functionalization, whereas the Pb system gave higher % C.L values.

Table 3 Effect of % weight of Pb salts on % grafting and % C.L

%Wt loading	Pb DA		Pb DMA	
	% Grafting	% C.L	% Grafting	% C.L
1	35.5	8.6	28.1	12.8
2	41.3	12.5	32.6	19.4
3	47.8	18.4	39.7	25.6
4	54.9	23.7	44.8	34.3
5	61.4	30.1	52.3	42.8

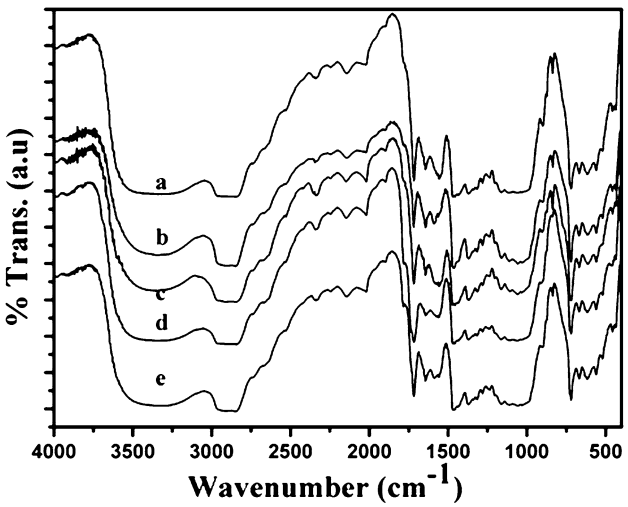

Fig. 11 FTIR spectra of LLDPE loaded with Sr DA at *a* 1 wt%, *b* 2 wt%, *c* 3 wt%, *d* 4 wt%, *e* 5 wt%

Table 4 Effect of % weight of Sr salts on % grafting and % C.L

%Wt loading	Sr DA		Sr DMA	
	% Grafting	% C.L	% Grafting	% C.L
1	52.3	3.7	45.7	5.4
2	58.6	6.4	47.8	11.1
3	61.4	9.8	52.4	18.6
4	67.1	14.4	55.6	26.8
5	75.3	20.2	60.1	35.7

Figure 11 shows the FTIR spectra of 1–5 wt% Sr DA-loaded LLDPE system. Here also the RI of [C=O/C–H]

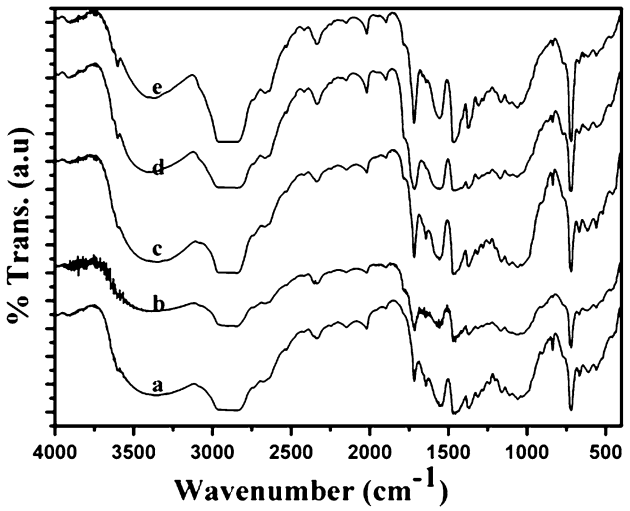

Fig. 12 FTIR spectra of LLDPE loaded with Sr DMA at *a* 1 wt%, *b* 2 wt%, *c* 3 wt%, *d* 4 wt%, *e* 5 wt%

was increased with the increase in % weight of Sr DA. This confirmed the chemical grafting of Sr DA onto LLDPE backbone. The order of functionalization reaction can be determined by drawing a plot of log(% weight of DCP) versus log($RI_{[C=O/C-H]}$) (Fig. 7e). The plot yielded a straight line with the slope value of 1.14, i.e. $R_f \propto (\%\ \text{weight of DCP})^{1.14}$. The slope value confirmed the 1.25 order of functionalization reaction with respect to % weight of DCP. The % grafting and % C.L values are given in Table 4. Figure 12 showed the FTIR spectrum of 1–5 wt% Sr DMA-loaded LLDPE system. The order of functionalization reaction was determined by plotting log(% weight of DCP) versus log($RI_{[C=O/C-H]}$) (Fig. 7f) as 1.76, i.e. $R_f \propto (\%\ \text{weight of DCP})^{1.76}$. This inferred that 1.75 mol of Sr DMA is required to functionalize 1 mol of LLDPE. On comparison, the Sr DA system gave higher % grafting due to smaller in size without steric effect and Sr DMA system

Scheme 1 Melt functionalization of metal salt with LLDPE

Initiation

LLDPE + DCP + Metal salt ⇌ Composite (C_1)

Composite (C_1) $\xrightarrow{\triangle}$ LLDPE + Metal salt + DCP#

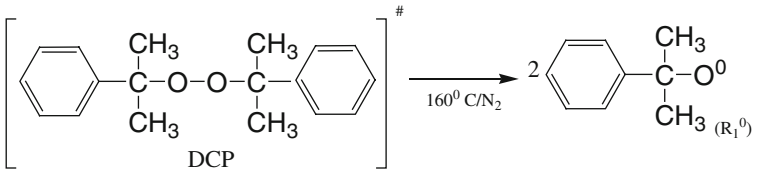

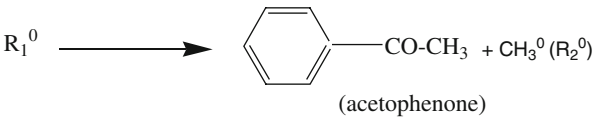

Propagation

R_1^0/R_2^0 + LLDPE ⟶ $LLDPE^0$ (R_3^0) + R_1H/R_2H

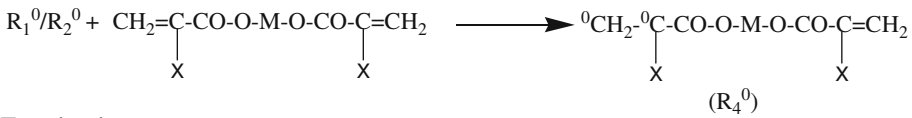

Termination

2 R_3^0 ⟶ LLDPE-LLDPE (cross linking)

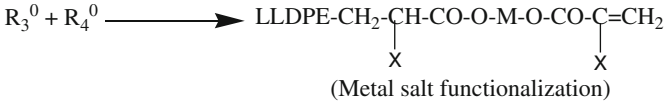

X=H, acrylate
X=CH_3, methacrylate

M=Cd^{2+}, Pb^{2+}, Sr^{2+}

yielded higher % C.L values due to the presence of steric effect [36] and slow formation of Sr DMA radicals. Table 4 exhibited the % grafting as well as % C.L values.

In overall comparison, Sr-containing divinyl monomers yielded higher % grafting due to the small size and absence of steric effect. The Pb-containing monomers gave higher % C.L values due to the presence of steric effect and very slow production of radicals. These results inferred that both grafting and C.L efficiency depended not only on the size and steric effect, but also depended on the melting temperature and miscible behaviour of monomer with LLDPE in its molten state.

Melt grafting mechanism

Anbarasan et al. [34] explained the mechanism of free radical grafting of thioester onto HDPE backbone. Similar type of mechanism is applied to the present system. However, the presence of two double bonds at the ends leads to different possible reactions. Melt functionalization reaction proceeds via free radical reaction. Free radical reactions precede through three steps namely initiation, propagation and termination reactions.

DCP, the free radical initiator, produced two cumyloxy radicals on heating at 160 °C with normal dissociation rate. Formations of free radicals are the initiation step of melt functionalization reaction. The formed free radicals interacted with LLDPE and other esters led to the various processes. In this investigation, we had used 1:1:1 ratio of LLDPE, esters and DCP. In general, 1 mol of DCP is required to initiate 1 mol of LLDPE and 1 mol of ester. Hence, we used the equal concentrations of DCP and ester. Coupling of LLDPE macroradicals led to the C.L reactions (Scheme 1).

Conclusions

From the above kinetic study, the important points are presented here as conclusions. The DAs yielded higher % functionalization and DMAs produced higher % C.L values. The Sr salts exhibited higher $T_{d.w}$, $T_{c.c}$ and % functionalization values due to smaller in size and with the outmost configuration of $5s^2$. The Pb DA retained 54.5 wt% residue above 750 °C. The Sr DA showed 1.14 order of functionalization, whereas Sr DMA showed 1.76 order of functionalization with respect to % weight of Sr salts. The Pb DA represented the highest crystallinity among the metal ion containing divinyl monomers. The FTIR spectral results declared that one double bond of metal esters were involved in the functionalization process and the other one was as such. The $RI_{[C=O/C-H]}$ was increased with the increase in % weight of metal salts due to more and more chemical grafting onto LLDPE backbone in the presence of DCP under inert atmosphere at 160 °C.

Acknowledgement The authors gratefully acknowledge the financial support by DST, New Delhi (Ref. No. SR/FTP/CS-39/2005).

References

1. Savostyanov VS, Pomogailo AD, Kristskaya DA, Ponomarew AN (1989) J Polym Sci A Polym Chem 27:1935
2. Costaschuk FM, Gilson DFR, St. Pierre LE (1971) Macromolecules 4:333
3. Pittman CU Jr, Voges RL, Jones WR (1971) Macromolecules 4:291
4. Pittman CU Jr, Voges RL, Jones WR (1971) Macromolecules 4:298
5. Gronowski A, Wojtczak Z (1989) Makromol Chem 190:2063
6. Peng Z, Liang X, Zhang Y, Zhang Y (2002) J Appl Polym Sci 84:1339
7. Iketa R, Yamada B, Tsuji M, Sakurai S (1999) Polym Int 48:446
8. Lu Y, Liu L, Tian M, Geng H, Zhang L (2005) Eur Polym J 111:589. doi:10.1016/j.eurpolymj.2004.10.012
9. Yamada B, Yoneo H, Otsu T (1970) J Polym Sci A-1 8:2021
10. Vaysse C, Demorgues LG, Duget E, Delmas C (2003) Inorg Chem 42:4559. doi:10.1021/ic.0262-295
11. Sayyah SM, Khaled MA, Sabry AI, Sabbah IA (1989) Acta Polym 40:293
12. Pookuik PK, Abzaeva KA, Voronkov MG (2008) Doklady Chem 418:8. doi:10.1134/S00125008080-10035
13. Cui F, Zhang J, Cui T, Liang S, Li B, Lin Q, Yang B (2008) Nano Res 1:195. doi:10.1007/s12279-8019-2
14. O'Donnell JH, McGarvey B, Morawetz H (1964) J Am Chem Soc 86:2322. doi:10.1021/ja010066a002
15. Sadeghi SMT (2005) Iran Polym J 14:657
16. Walker EH, Apblett AW, Walker R, Zachary A (2009) Chem Mater 16:5336. doi:10.1029/cm0489385
17. Duxin N, Liu F, Vali H, Eisenberg A (2005) J Am Chem Soc 127:10063. doi:10.1029/ja0505043
18. Khanna PK, Charan S, Viswanath AK (2006) Mater Chem Phys 97:288. doi:10.1016/j.matchemphys.2005.08.012
19. Huang LP, Zhou XP, Tong SY (2008) J Mater Sci 43:4290. doi:10.1007/s10853-008-2626-x
20. Anbarasan R, Sudha M, Dhanalakshmi V (2010) Appl Spect (submitted)
21. Wang JS, Shi JS, Wu JG (2003) World J Gastrol 9:1897
22. Xueref I, Domine F (2003) Atmos Chem Phys 3:1779
23. Rathika S, Baskaran I, Anbarasan R (2009) J Mater Sci 44:3542. doi:10.1007/s10853-009-3478-8
24. Duraimurugan K, Rathika S, Anbarasan R (2008) Chin J Polym Sci 26:393. doi:10.1142/S0256767908003059
25. Saule M, Navarre S, Babot O, Maillard B (2003) Macromolecules 36:7469. doi:10.1021/ma0342325
26. Saule M, Navarre S, Babot O, Maillard B (2005) Macromolecules 38:77. doi:10.1021/ma048712n
27. Navarre S, Maillard B (2000) J Polym Sci A Polym Chem 38:2957
28. Parveen MF, Dhanalakshmi V, Anbarasan R (2009) J Mater Sci 44:5852. doi:10.1007/s10853-009-3826-8
29. Parveen MF, Dhanalakshmi V, Anbarasan R (2009) NANO 4:147
30. Yelilarasi A, Juliat Latha Jayakumari J, Anbarasan R (2009) Spectrochim Acta A 74:1229. doi:10.1016/j.saa.2009.09.042
31. Yelilarasi A, Juliat Latha Jayakumari J, Anbarasan R (2009) Polym Polym Compos 17:397

32. Anbarasan R, Kanchana S, Gayathri S, Jayalakshmi T, Dhanalakshmi V (2010) J Appl Polym Sci 115:315. doi:101002/app.31120
33. Anbarasan R, Dhanalakshmi V, Rajasulochana K, Sudha M, Jayalakshmi T, Anusuya M (2010) J Appl Polym Sci 115:2582. doi:10.1002/app.31257
34. Anbarasan R, Babout O, Maillard B (2005) J Appl Polym Sci 97:761. doi:10.1002/app.21342
35. Anbarasan R, Babout O, Dequil M, Maillard B (2005) J Appl Polym Sci 97:766. doi:10.1002/app.21343
36. Parthasarathi V, Dhanalakshmi V, Anbarasan R (2010) Polym Eng Sci 50:474. doi:10.1002/pen.21546